PHYSICAL REVIEW E **105**, 065114 (2022)

Effective temperature and Einstein relation for particles in active matter flows

Sanjay C. P. and Ashwin Joy *

Department of Physics, Indian Institute of Technology Madras, Chennai 600036, India

(Received 23 September 2021; accepted 9 June 2022; published 30 June 2022)

Active matter are a collection of units with intrinsic supply of energy that is utilized for self-propelled motion. Recent studies have confirmed that these active systems can exist in exotic phases, such as swarming, laning, jamming, and even turbulence, based on the size and density of the constituent units. An interesting question that naturally arises is whether one can identify an effective temperature for particles advected by such an active flow that is far from equilibrium. In this paper, we report using a continuum model of a dense bacterial suspension, an exact expression of the effective temperature for a distribution of interacting particles that are immersed in this suspension. We observe that this effective temperature is linear in particle diffusivity with the slope defining the particle mobility that is higher when the background fluid exhibits global polar ordering and lower when the fluid is in isotropic equilibrium. We believe our paper is a direct verification of the Einstein relation—the simplest fluctuation dissipation relation for interacting particles advected in an active matter flow.

DOI: 10.1103/PhysRevE.105.065114

I. INTRODUCTION

Active matter is a fascinating nonequilibrium system whose constituent units have an intrinsic source of energy that is capable of generating persistent motion. Familiar examples for these systems are bacterial suspensions [1,2], microtubule networks [3], artificial swimmers [4], and active liquid crystals [5] to mention a few. It is well known that the inherent activity of the constituent particles can lead to the formation of beautiful patterns [6–9]. In particular, recent studies have shown that bacterial suspensions can exist in a variety of exotic phases, such as swarming, laning, jamming, and even turbulence based on the size and density of the individual units [10]. There is extensive literature on particle transport in such active suspensions where activity was shown to enhance the diffusivity and mixing of particles[11–22]. It is, therefore, natural to ask whether one can describe an effective temperature for particles are advected by such active flows [23,24]. A related and important question is whether these active fluids that are essentially far from equilibrium, should satisfy fluctuation-dissipation relations (FDR) even in the absence of detailed balance [25,26]. There are some important works showing that FDRs can be derived without detailed balance as long as some invariant measure exists in the system [27,28]. In this paper, we address this fundamental issue by analytically and numerically investigating the motion of a distribution of interacting particles in a dense suspension of bacteria, the latter described by a recently developed continuum model. Our simulations confirm that the invariant measures of velocity distribution of both the background flow as well as the particles obey Gaussian statistics directly suggesting the existence of a FDR III. We also provide an exact theoretical expression for the effective temperature by solving the Fokker-Planck equations corresponding to the governing equations of the particles. Our prediction, that does not invoke any free parameters, matches very well with the numerically estimated variance of the velocity distribution. Quite interestingly, this effective temperature is found to be linear in particle diffusivity with the slope characterizing the particle mobility, that is higher when the background fluid exhibits global polar ordering, and lower when the fluid is in isotropic equilibrium. Our paper is, therefore, a direct verification of the celebrated Einstein relation—the simplest FDR, for interacting particles advected in an active flow. The results reported here are valid across four decades of variation in the damping coefficient thereby putting a large number of active systems within the ambit of our paper—from dense suspensions of microswimmers that are traditionally overdamped [9,29,30] to the lesser understood underdamped suspensions where inertial effects are significant, notable examples being ciliates, planktons, copepods, and other macroswimmers moving in a background media of low viscosity [31]. Significance of effective temperature in biologically relevant systems have been known from the studies of active processes in hair bundles [32], gene networks [33], and the stability of different phases of motorized particle systems [34]. Earlier experiments conducted to understand the motion of beads in suspensions of bacteria have already suggested the possibility of an effective temperature which is several times larger than that of a classical Brownian particle [35]. Our paper should also find applications in the field of micrometer sized heat engines where bacterial suspensions are used as temperature reservoirs [36,37]. In what follows, we discuss the model and methods in Sec. II, theoretical investigation in Sec. III, and a summary of our results in Sec. IV.

II. MODEL AND METHODS

To mimic a generic active suspension, we use a minimal continuum model [10,38] of an active fluid that is known to predict velocity statistics and correlations observed in

*ashwin@physics.iitm.ac.in

laboratory experiments on suspensions of bacteria *Bacillus subtilis* with excellent accuracy [39]. In two dimensions, the incompressible velocity field $\boldsymbol{u}(\boldsymbol{x}, t)$ in this model evolves according to the following equations,

$$\frac{\partial \boldsymbol{u}}{\partial t} + \lambda_0(\boldsymbol{u}\cdot\nabla)\boldsymbol{u} = -\nabla P - \Gamma_0\nabla^2\boldsymbol{u} - \Gamma_2\nabla^4\boldsymbol{u} - \mu\boldsymbol{u},$$
$$\nabla\cdot\boldsymbol{u} = 0, \tag{1}$$

where the nondimensional parameter λ_0 decides the type of active unit, meaning they are either *pusher* (e.g., *Bacillus subtilis, E. coli*) or a *puller* (e.g., *C. reinhardtii*), corresponding, respectively, to the case $\lambda_0 > 0$ or $\lambda_0 < 0$. The model was recently used to investigate pattern formation [40] and transport coefficients in dense active fluids [22]. We set the value of $\lambda_0 = 3.5$ throughout our paper implying that we have a *pusher* type of active units. We keep $\Gamma_0 > 0$ to enable energy injection into the active fluid via instabilities, driving a "turbulent" or high-dimensional chaotic flow, whereas $\Gamma_2 > 0$ stabilizes the flow at high wave numbers. The scalar field $\mu = \alpha + \beta|\boldsymbol{u}|^2$ depends on the local velocity $\boldsymbol{u}$ and was first introduced by Toner and Tu [41] and Toner *et al.* [7] to model the "flocking" behavior in self-propelled rodlike objects. The parameter α, henceforth, referred to as the Ekman friction, acts at intermediate scales and can either lead to a damping of energy when $\alpha > 0$ or an injection of energy when $\alpha < 0$. Former leads the fluid to an isotropic equilibrium and the latter yields a globally ordered polar state with mean velocity $\sqrt{|\alpha|/\beta}$. To nondimensionalize Eq. (1), we normalize all distances to a characteristic length $\sigma_0 = 5\pi\sqrt{2\Gamma_2/\Gamma_0}$ and all times to $t_0 = 5\pi\sqrt{2}\Gamma_2/\Gamma_0^2$. In terms of these reduced units, we fix the values of the model parameters as $\Gamma_0 = (5\pi\sqrt{2})^{-1}$, $\Gamma_2 = (5\pi\sqrt{2})^{-3}$, and $\beta = 0.5$, in order to remain consistent with earlier works [22,42,43]. Following Wensink *et al.* [10], we identify Γ_2/Γ_0^2 as the timescale for the growth of linear instabilities and $1/|\alpha|$ as the timescale for damping or acceleration effects. Equation (1) is then numerically solved using a pseudo-spectral approach over a square grid of 512^2 points in a doubly periodic box of size 2π. We overcome the aliasing errors that arise due to the implementation of discrete Fourier transforms by performing 2/3 and 1/2 dealiasing rules, respectively, for the quadratic $[(\boldsymbol{u}\cdot\nabla)\boldsymbol{u}]$ and cubic $[(|\boldsymbol{u}|^2)\boldsymbol{u}]$ terms [44]. Time marching of $\boldsymbol{u}$ is performed using the Crank-Nicolson scheme with a time step of $\Delta t = 2\times10^{-4}$ that is sufficient to maintain numerical stability in the entire range of parameters explored here.

Into the active flow, we throw N particles that follow the dynamics:

$$\frac{d\boldsymbol{r}_i}{dt} = \boldsymbol{v}_i,$$
$$\frac{d\boldsymbol{v}_i}{dt} = -\gamma[\boldsymbol{v}_i - \boldsymbol{u}(\boldsymbol{r}_i)] - \nabla_i\Phi, \tag{2}$$

where γ is the damping coefficient and $(\boldsymbol{r}_i, \boldsymbol{v}_i)$ correspond, respectively, to position and velocity of an ith particle. We realize $\boldsymbol{u}(\boldsymbol{r}_i)$ as the active flow field projected at the location of this particle which is obtained using cubic spline interpolation [45] and $-\nabla_i\Phi$ as the mass normalized force acting on it. The limit $\gamma \longrightarrow \infty$ naturally corresponds to an overdamped dynamics of passive tracers advected by a background flow.

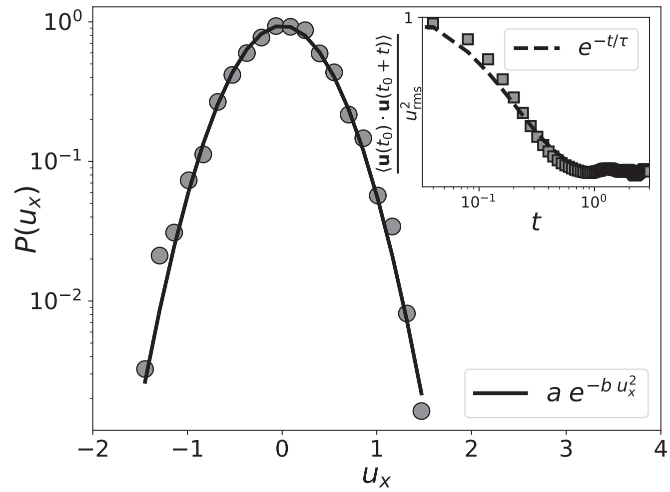

FIG. 1. Distribution of Eulerian velocities projected on the particles fits well to a Gaussian (solid line) with parameters $a = 1.13$ and $b = 4.75$. Data shown here correspond to $\alpha = 3$; results are similar for other α's. The inset: Temporal autocorrelation of $\boldsymbol{u}$ decays exponentially with a relaxation time $\tau = 0.21t_0$. We can, thus, visualize $\boldsymbol{u}$ as a Gaussian colored noise—a headway that will be used to formulate an effective temperature for our particles.

In this limit, the tracers can exhibit an intervening anomalous diffusive regime [46] as the Ekman friction is pushed to negatively larger values, say $\alpha < -6$. The limit $\gamma \longrightarrow 0$ on the other hand, corresponds to the Newtonian dynamics of particles without any background fluid. At intermediate values of γ, both inertial and damping effects coexist thereby rendering generality to the particle dynamics. We set the interaction between particles as the repulsive Weeks-Chandler-Andersen potential energy $\Phi = \sum_{j<k}\phi(|\boldsymbol{r}_j - \boldsymbol{r}_k|)$ where the potential,

$$\phi(r) = \begin{cases} 4\epsilon\Big[\Big(\frac{\sigma_0}{r}\Big)^{12} - \Big(\frac{\sigma_0}{r}\Big)^{6}\Big] + \epsilon, & r < 2^{1/6}\sigma_0, \\ 0, & r > 2^{1/6}\sigma_0, \end{cases} \tag{3}$$

with σ_0 as the characteristic length (defined above) and ϵ is a scale with dimension energy per unit mass that sets the particle interactions. All measurements on the particles as well as the active fluid are carried out only after the latter attains a steady state. To improve our statistics, we average these measurements over 100 independently prepared realizations of the initial state. Below we show that the statistics of the Eulerian velocity $\boldsymbol{u}$ is indeed profitable to the prediction of an effective temperature of our particles.

III. THEORY

A. Statistics of $\boldsymbol{u}$

We start with a measurement of the Eulerian flow field projected at the particle positions, i.e., $\boldsymbol{u}(\boldsymbol{r}_i)$. In Fig. 1, we show the distribution of a component of this velocity in the steady state and realize that it is well approximated by a Gaussian. These numerical observations strongly suggest the existence of a FDR as the Gaussian statistics can be used to invoke a generalized time reversal transformation that may restore detailed balance [47,48]. In the Fig. 1 inset, we show that the temporal autocorrelation of $\boldsymbol{u}$ is clearly an exponential with a relaxation time τ. We combine the foregoing facts to assert that the fluid velocity projected at particle locations is essentially a Gaussian colored noise of zero mean and variance given as

$$\langle u_{i\chi}(t)u_{j\psi}(t')\rangle = (1/2)\delta_{ij}\delta_{\chi\psi}u_{\rm rms}^2\exp(-|t-t'|/\tau), \quad (4)$$

where $u_{\rm rms}$ is a velocity scale that sets the kinetic energy of the background fluid in the steady state. The relaxation time τ can also be obtained from the fluid properties directly as $\ell^*/u_{\rm rms}$ where ℓ^* is the mean vortex size [22]. We use the Latin symbols i, j to denote particle labels and the Greek symbols χ, ψ to denote spatial indices. In light of all these arguments, we realize that the stochastic dynamics in Eq. (2) is essentially non-Markovian and its corresponding steady state Fokker-Planck equation must be carefully solved (see next) to derive an exact expression of the stationary probability distribution. Factorization of this distribution into position and momentum parts will yield an exact expression of the effective temperature of our particles. This is performed next.

B. Theoretical prediction of $T_{\rm eff}$

To systematically derive an expression for the effective temperature $T_{\rm eff}$ in terms of the fluid properties, we will now set up a Fokker-Planck equation for the governing dynamics of the interacting particles and solve it to get a stationary velocity distribution. As stated earlier, the dynamics shown in Eq. (2) is essentially non-Markovian due to the Gaussian colored noise $\boldsymbol{u}$. An exact solution of the corresponding Fokker-Planck equation with the exception of harmonic interactions is intractable in the general case, and approximations are always required [49]. To circumvent this difficulty, we reduce the original non-Markovian dynamics in Eq. (2) to an equivalent Markovian dynamics by an appropriate enlargement of the phase space [50,51]. In the component form, this simply reads

$$\begin{aligned}\frac{dr_{i\chi}}{dt} &= v_{i\chi},\\ \frac{dv_{i\chi}}{dt} &= -\gamma(v_{i\chi}-u_{i\chi}) - \nabla_{i\chi}\Phi,\\ \frac{du_{i\chi}}{dt} &= -\frac{1}{\tau}u_{i\chi} + \sqrt{\frac{u_{\rm rms}^2}{\tau}}\xi_{i\chi}, \end{aligned}\quad (5)$$

where $\boldsymbol{\xi}_i$ is a Gaussian white noise with zero mean and correlation $\langle\xi_{i\chi}(t)\xi_{j\psi}(t')\rangle = \delta_{ij}\delta_{\chi\psi}\delta(t-t')$. The reader should note that the dynamics in Eq. (6) is consistent with the expected correlation properties of $\boldsymbol{u}$ that we already know from Eq. (4). The Fokker-Planck equation for the probability distribution $\mathcal{P}(r_\chi, v_\chi, t)$ corresponding to the dynamics in (6) can be written using a decoupling approximation as [52]

$$\frac{\partial}{\partial t}\mathcal{P}(r_\chi, v_\chi, t) = \mathcal{L}\mathcal{P}(r_\chi, v_\chi, t), \quad (6)$$

where the operator $\mathcal{L}$ is defined as

$$\mathcal{L} = \left[-v_\chi\frac{\partial}{\partial r_\chi} + \frac{\partial}{\partial v_\chi}\left(\gamma v_\chi + \frac{\partial\Phi}{\partial r_\chi}\right) + \frac{\gamma^2 u_{\rm rms}^2\tau}{2\left(1+\gamma\tau+\tau^2\left\langle\frac{\partial^2\Phi}{\partial r_\chi^2}\right\rangle\right)}\frac{\partial^2}{\partial v_\chi^2} + \frac{\gamma^2u_{\rm rms}^2\tau^2}{2\left(1+\gamma\tau+\tau^2\left\langle\frac{\partial^2\Phi}{\partial r_\chi^2}\right\rangle\right)}\frac{\partial^2}{\partial r_\chi\partial v_\chi}\right], \quad (7)$$

The steady state solution of the above Fokker-Planck equation readily factorizes into position and velocity parts as

$$\mathcal{P}_{\rm s}(r_\chi, v_\chi) = \frac{1}{\mathcal{Z}}\exp\left(-\frac{v_\chi^2}{2\sigma_\chi^2}\right)\exp\left[-\frac{\Phi}{\sigma_\chi^2(1+\gamma\tau)}\right], \quad (8)$$

with the velocity variance realized as

$$\sigma_\chi^2 = \frac{u_{\rm rms}^2\gamma\tau}{2\left(1+\gamma\tau+\tau^2\left\langle\frac{\partial^2\Phi}{\partial r_\chi^2}\right\rangle\right)} \equiv T_{\rm eff}, \quad (9)$$

the effective temperature of our inertial particles with χ being x or y. We take a moment of pause to appreciate the beauty of this exact expression. There are no fitting parameters here, and we are able to completely predict the effective temperature of particles once the background fluid properties ($u_{\rm rms}, \tau, \gamma$) and particle interactions (Φ) are specified. The predicted $T_{\rm eff}$ is in excellent agreement with the numerically estimated value that is obtained by fitting the velocity distribution to a Gaussian. This is shown in Fig. 2 where we plot $T_{\rm eff}$ vs D, the particle diffusivity. For each γ, we calculate the diffusivity as $D = \lim_{t\to\infty}\langle\Delta r^2\rangle/(4t)$ and its variation $D_{\rm min} \to D_{\rm max}$ comes from varying the fluid friction α in the range of 4.0 to -4.0. It is evident from each panel of this figure that $T_{\rm eff}$ is linear in D with a slope yielding the inverse of particle mobility μ. This is a direct verification of Einstein's relation, the simplest formulation of FDR. We also observe that the particle mobility is higher when the background fluid is in a globally ordered polar state, i.e., $\alpha < 0$, and lower when the fluid is in isotropic equilibrium or $\alpha > 0$. Our results are valid across four decades of variation in the damping coefficient effectively covering the entire range $1 < \gamma\tau < 10^4$, where the lower and upper limits corresponding, respectively, to the inertial and overdamped regimes. This puts a large number of active systems within the purview of our paper—from overdamped suspensions of microswimmers [35,53] to the underdamped suspensions of macroswimmers, such as ciliates, planktons, and copepods moving in low viscosity media [31]. We would like to mention the range of densities explored $\rho = 0.6$–0.8 correspond to a physical range of 6×10^4–$8\times10^4/\text{cm}^2$ that is typically encountered in laboratory experiments, such as Ref. [35]. At higher densities, we observe that the particle velocity exhibit deviation from Gaussian behavior putting that range outside the ambit of our paper.

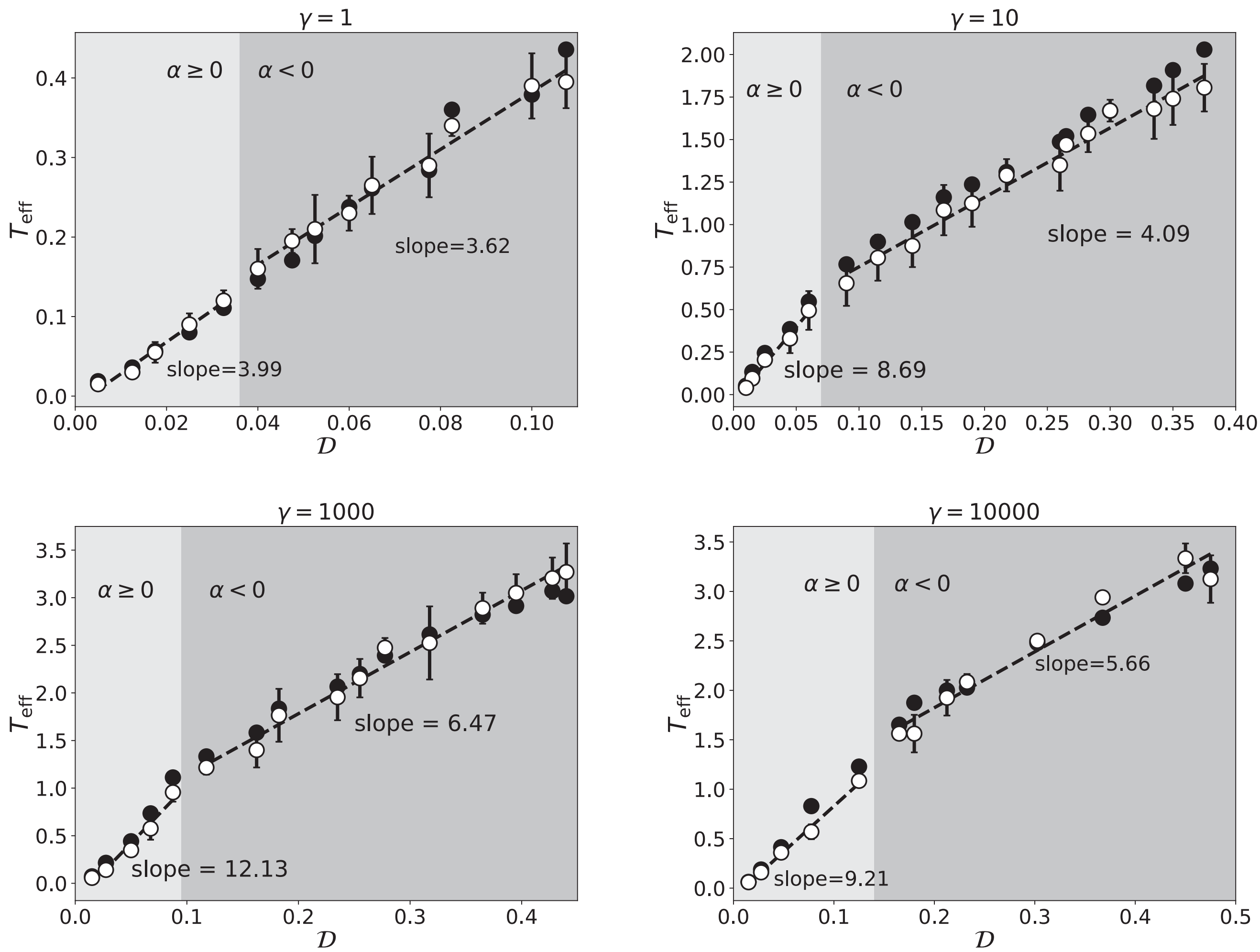

FIG. 2. Evidence of the linear relationship between effective temperature $T_{\rm eff}$ and particle diffusivity D is presented here at various value of damping coefficient γ. The numerical value of $T_{\rm eff}$ is extracted by fitting the distribution of $\boldsymbol{v}$ to a Gaussian (empty circles:○) and the theoretical value is predicted by Eq. (9) (filled circles:). The error bars represent one standard deviation in the numerical estimate. The dashed line is a linear fit to our numerical data and has a slope that indicates the inverse of particle mobility μ. This is a direct verification of Einstein's relation, the simplest FDR. Particle diffusivity $D = \lim_{t\to\infty}\langle\Delta r^2\rangle/(4t)$ is varied by varying the fluid friction α. For each panel that corresponds to a specific γ, the mobility of particles is higher when the background fluid is in a globally ordered polar state ($\alpha < 0$), and lower when it is in isotropic equilibrium ($\alpha > 0$). The former corresponds to energy injection by the friction term in Eq. (1), and the latter corresponds to the damping of energy. These two regimes have been shown in different shades to clearly demonstrate the change in the mobility of the particles.

IV. SUMMARY

We have demonstrated that a distribution of interacting particles immersed in an active fluid can be described by an effective temperature. To achieve this, we solved the steady state Fokker-Planck equation corresponding to the stochastic governing equations of the particles. The result is an exact relation between the effective temperature, properties of the background flow, and particle interactions. Finally we show this effective temperature is linear in particle diffusivity with the slope characterizing particle mobility. This is a direct verification of the Einstein's relation—the simplest FDR, for particles advected by a dense bacterial flow. The mobility is observed to be higher when the background fluid is in a globally ordered polar phase and lower when the fluid is in isotropic equilibrium. The results reported here apply to active fluids prepared under a broad spectrum of particle damping and are, therefore, general in nature.

ACKNOWLEDGMENTS

We thank V. Balakrishnan, S. Thampi, and A. Sen for discussions and comments on the paper. All simulations were performed on the HPC-Physics cluster of our group. Support from the SERB core Grant SP20210716PHSERB008690, DST, and New Faculty Seed Grant (NFSG) PHY1819707NFSCASHN, IIT Madras, is gratefully acknowledged.

[1] C. Dombrowski, L. Cisneros, S. Chatkaew, R. E. Goldstein, and J. O. Kessler, Self-Concentration and Large-Scale Coherence in Bacterial Dynamics, Phys. Rev. Lett. **93**, 098103 (2004).
[2] T. Ishikawa, N. Yoshida, H. Ueno, M. Wiedeman, Y. Imai, and T. Yamaguchi, Energy Transport in a Concentrated Suspension of Bacteria, Phys. Rev. Lett. **107**, 028102 (2011).
[3] T. Sanchez, D. T. N. Chen, S. J. DeCamp, M. Heymann, and Z. Dogic, Spontaneous motion in hierarchically assembled active matter, Nature (London) **491**, 431 (2012).
[4] D. Nishiguchi and M. Sano, Mesoscopic turbulence and local order in janus particles self-propelling under an ac electric field, Phys. Rev. E **92**, 052309 (2015).
[5] R. Alert, J.-F. Joanny, and J. Casademunt, Universal scaling of active nematic turbulence, Nat. Phys. **16**, 682 (2020).
[6] R. A. Simha and S. Ramaswamy, Hydrodynamic Fluctuations and Instabilities in Ordered Suspensions of Self-Propelled Particles, Phys. Rev. Lett. **89**, 058101 (2002).
[7] J. Toner, Y. Tu, and S. Ramaswamy, Hydrodynamics and phases of flocks, Ann. Phys. (NY) **318**, 170 (2005).
[8] S. Ramaswamy, The mechanics and statistics of active matter, Annu. Rev. Condens. Matter Phys. **1**, 323 (2010).
[9] M. C. Marchetti, J. F. Joanny, S. Ramaswamy, T. B. Liverpool, J. Prost, M. Rao, and R. A. Simha, Hydrodynamics of soft active matter, Rev. Mod. Phys. **85**, 1143 (2013).
[10] H. H. Wensink, J. Dunkel, S. Heidenreich, K. Drescher, R. E. Goldstein, H. Löwen, and J. M. Yeomans, Meso-scale turbulence in living fluids, Proc. Natl. Acad. Sci. USA **109**, 14308 (2012).
[11] K. C. Leptos, J. S. Guasto, J. P. Gollub, A. I. Pesci, and R. E. Goldstein, Dynamics of Enhanced Tracer Diffusion in Suspensions of Swimming Eukaryotic Microorganisms, Phys. Rev. Lett. **103**, 198103 (2009).
[12] C. Valeriani, M. Li, J. Novosel, J. Arlt, and D. Marenduzzo, Colloids in a bacterial bath: simulations and experiments, Soft Matter **7**, 5228 (2011).
[13] G. Miño, T. E. Mallouk, T. Darnige, M. Hoyos, J. Dauchet, J. Dunstan, R. Soto, Y. Wang, A. Rousselet, and E. Clement, Enhanced Diffusion due to Active Swimmers at a Solid Surface, Phys. Rev. Lett. **106**, 048102 (2011).
[14] A. Lagarde, N. Dagès, T. Nemoto, V. Démery, D. Bartolo, and T. Gibaud, Colloidal transport in bacteria suspensions: from bacteria collision to anomalous and enhanced diffusion, Soft Matter **16**, 7503 (2020).
[15] T. M. Squires and J. F. Brady, A simple paradigm for active and nonlinear microrheology, Phys. Fluids **17**, 073101 (2005).
[16] P. T. Underhill, J. P. Hernandez-Ortiz, and M. D. Graham, Diffusion and Spatial Correlations in Suspensions of Swimming Particles, Phys. Rev. Lett. **100**, 248101 (2008).
[17] D. O. Pushkin and J. M. Yeomans, Fluid Mixing by Curved Trajectories of Microswimmers, Phys. Rev. Lett. **111**, 188101 (2013).
[18] Z. Lin, J.-L. Thiffeault, and S. Childress, Stirring by squirmers, J. Fluid Mech. **669**, 167 (2011).
[19] A. Morozov and D. Marenduzzo, Enhanced diffusion of tracer particles in dilute bacterial suspensions, Soft Matter **10**, 2748 (2014).
[20] J.-L. Thiffeault, Distribution of particle displacements due to swimming microorganisms, Phys. Rev. E **92**, 023023 (2015).
[21] E. W. Burkholder and J. F. Brady, Tracer diffusion in active suspensions, Phys. Rev. E **95**, 052605 (2017).
[22] S. C. P. and A. Joy, Friction scaling laws for transport in active turbulence, Phys. Rev. Fluids **5**, 024302 (2020).
[23] L. F. Cugliandolo, The effective temperature, J. Phys. A: Math. Theor. **44**, 483001 (2011).
[24] A. Puglisi, A. Sarracino, and A. Vulpiani, Temperature in and out of equilibrium: A review of concepts, tools and attempts, Phys. Rep. **709-710**, 1 (2017).
[25] L. Caprini, A. Puglisi, and A. Sarracino, Fluctuation–dissipation relations in active matter systems, Symmetry **13**, 81(2021).
[26] D. Martin, J. O'Byrne, M. E. Cates, É. Fodor, C. Nardini, J. Tailleur, and F. van Wijland, Statistical mechanics of active ornstein-uhlenbeck particles, Phys. Rev. E **103**, 032607 (2021).
[27] R. F. Fox and G. E. Uhlenbeck, Contributions to non-equilibrium thermodynamics. I. theory of hydrodynamical fluctuations, Phys. Fluids **13**, 1893 (1970).
[28] R. Graham, Covariant formulation of non-equilibrium statistical thermodynamics, Z Phys. B: Condens. Matter Quanta **26**, 397 (1977).
[29] G. Gompper, R. G. Winkler, T. Speck, A. Solon, C. Nardini, F. Peruani, H. Löwen, R. Golestanian, U. B. Kaupp, L. Alvarez, T. Kiørboe, E. Lauga, W. C. K. Poon, A. DeSimone, S. Muiños-Landin, A. Fischer, N. A. Söker, F. Cichos, R. Kapral, P. Gaspard *et al.*, The 2020 motile active matter roadmap, J. Phys.: Condens. Matter **32**, 193001 (2020).
[30] C. Bechinger, R. Di Leonardo, H. Löwen, C. Reichhardt, G. Volpe, and G. Volpe, Active particles in complex and crowded environments, Rev. Mod. Phys. **88**, 045006 (2016).
[31] D. Klotsa, As above, so below, and also in between: mesoscale active matter in fluids, Soft Matter **15**, 8946 (2019).
[32] P. Martin and A. J. Hudspeth, Active hair-bundle movements can amplify a hair cell's response to oscillatory mechanical stimuli, Proc. Natl. Acad. Sci. USA **96**, 14306 (1999).
[33] T. Lu, J. Hasty, and P. G. Wolynes, Effective temperature in stochastic kinetics and gene networks, Biophys. J. **91**, 84 (2006).
[34] T. Shen and P. G. Wolynes, Stability and dynamics of crystals and glasses of motorized particles, Proc. Natl. Acad. Sci. USA **101**, 8547 (2004).
[35] X.-L. Wu and A. Libchaber, Particle Diffusion in a Quasi-Two-Dimensional Bacterial Bath, Phys. Rev. Lett. **84**, 3017 (2000).
[36] S. Krishnamurthy, S. Ghosh, D. Chatterji, R. Ganapathy, and A. K. Sood, A micrometre-sized heat engine operating between bacterial reservoirs, Nat. Phys. **12**, 1134 (2016).
[37] N. Roy, N. Leroux, A. K. Sood, and R. Ganapathy, Tuning the performance of a micrometer-sized stirling engine through reservoir engineering, Nat. Commun. **12**, 1 (2021).
[38] J. Dunkel, S. Heidenreich, M. Bär, and R. E. Goldstein, Minimal continuum theories of structure formation in dense active fluids, New J. Phys. **15**, 045016 (2013).
[39] J. Dunkel, S. Heidenreich, K. Drescher, H. H. Wensink, M. Bär, and R. E. Goldstein, Fluid Dynamics of Bacterial Turbulence, Phys. Rev. Lett. **110**, 228102 (2013).
[40] M. James, W. J. T. Bos, and M. Wilczek, Turbulence and turbulent pattern formation in a minimal model for active fluids, Phys. Rev. Fluids **3**, 061101(R) (2018).
[41] J. Toner and Y. Tu, Flocks, herds, and schools: A quantitative theory of flocking, Phys. Rev. E **58**, 4828 (1998).

[42] V. Bratanov, F. Jenko, and E. Frey, New class of turbulence in active fluids, Proc. Natl. Acad. Sci. USA **112**, 15048 (2015).

[43] M. James and M. Wilczek, Vortex dynamics and lagrangian statistics in a model for active turbulence, Eur. Phy. J. E: Soft Matter Biol. Phys. **41**, 21 (2018).

[44] C. Canuto, M. Y. Hussaini, A. Quarteroni, A. Thomas, Jr., *et al.*, *Spectral Methods in Fluid Dynamics* (Springer, Berlin, 2012).

[45] C. E. Pearson, *Numerical Methods in Engineering & science* (CRC, Boca Raton, FL, 1986).

[46] S. Mukherjee, R. K. Singh, M. James, and S. S. Ray, Anomalous Diffusion and Lévy Walks Distinguish Active from Inertial Turbulence, Phys. Rev. Lett. **127**, 118001 (2021).

[47] R. Graham, Solution of fokker planck equations with and without manifest detailed balance, Z. Phys. B: Condens. Matter Quanta **40**, 149 (1980).

[48] M. Ding, Z. Tu, and X. Xing, Covariant formulation of nonlinear langevin theory with multiplicative gaussian white noises, Phys. Rev. Research **2**, 033381 (2020).

[49] P. Hanggi and P. Jung, Colored Noise in Dynamical Systems, Adv. Chem. Phys. **89**, 239–326 (1995).

[50] N. G. Van Kampen, *Stochastic Processes in Physics and Chemistry*(Elsevier, Amsterdam, 1992), Vol. 1.

[51] H. Risken, Fokker-planck equation, in *The Fokker-Planck Equation* (Springer, Berlin, 1996) pp. 63–95.

[52] L. Fronzoni, P. Grigolini, P. Hanggi, F. Moss, R. Mannella, and P. V. E. McClintock, Bistable oscillator dynamics driven by nonwhite noise, Phys. Rev. A **33**, 3320 (1986).

[53] F. Kümmel, B. ten Hagen, R. Wittkowski, I. Buttinoni, R. Eichhorn, G. Volpe, H. Löwen, and C. Bechinger, Circular Motion of Asymmetric Self-Propelling Particles, Phys. Rev. Lett. **110**, 198302 (2013).